Kondo effect in quantum dots

2004 J. Phys.: Condens. Matter 16 R513

(http://iopscience.iop.org/0953-8984/16/16/R01)

INSTITUTE OF PHYSICS PUBLISHING JOURNAL OF PHYSICS: CONDENSED MATTER

J. Phys.: Condens. Matter **16** (2004) R513–R537 PII: S0953-8984(04)59608-X

TOPICAL REVIEW

Kondo effect in quantum dots

Michael Pustilnik[1] **and Leonid Glazman**[2]

[1] School of Physics, Georgia Institute of Technology, Atlanta, GA 30332, USA
[2] William I. Fine Theoretical Physics Institute, University of Minnesota, Minneapolis, MN 55455, USA

Received 30 January 2004
Published 8 April 2004
Online at stacks.iop.org/JPhysCM/16/R513
DOI: 10.1088/0953-8984/16/16/R01

Abstract

We review mechanisms of low-temperature electronic transport through a quantum dot weakly coupled to two conducting leads. Transport in this case is dominated by electron–electron interaction. At temperatures moderately lower than the charging energy of the dot, the linear conductance is suppressed by the Coulomb blockade. Upon further lowering of the temperature, however, the conductance may start to increase again due to the Kondo effect. We concentrate on lateral quantum dot systems and discuss the conductance in a broad temperature range, which includes the Kondo regime.

Contents

1. Introduction

In quantum dot devices [1] a small droplet of electron liquid is confined in a finite region of space. The droplet can be attached by tunnelling junctions to massive electrodes to allow electronic transport across the system. The conductance of such a device is determined by the number of electrons on the dot N, which in turn is controlled by varying the potential on the gate—an auxiliary electrode capacitively coupled to the dot [1]. At sufficiently low temperatures the number of electrons N is an integer at almost any gate voltage V_g. Exceptions are narrow intervals of V_g in which an addition of a single electron to the dot does not significantly change the electrostatic energy of the system. Such a degeneracy between different charge states of the dot allows for an activationless electron transfer through it, whereas for all other values of V_g the activation energy for the conductance G across the dot is finite. The resulting oscillatory dependence $G(V_g)$ is the hallmark of the Coulomb blockade phenomenon [1]. The contrast between the low- and high-conductance regions (Coulomb blockade valleys and peaks, respectively) gets sharper at lower temperatures. This pattern of $G(V_g, T)$ dependence is observed down to the lowest attainable temperatures in experiments on tunnelling through small metallic islands [2]. However, small quantum dots formed in GaAs heterostructures exhibit drastically different behaviour [3]: in some Coulomb blockade valleys the dependence $G(T)$ is not monotonic and has a minimum at a finite temperature. This minimum is similar in origin [4] to the well known non-monotonic temperature dependence of the resistivity of a metal containing magnetic impurities [5]—the *Kondo effect*.

In this paper we review the theory of the Kondo effect in quantum dots, concentrating on the so-called *lateral quantum dot systems* [1, 3], formed by gate depletion of a two-dimensional electron gas at the interface between two semiconductors. These devices offer the highest degree of tunability, yet allow for relatively simple theoretical treatment. At the same time, many of the results presented below are directly applicable to other systems as well, including vertical quantum dots [6–8], Coulomb-blockaded carbon nanotubes [8, 9], single-molecule transistors [10], and stand-alone magnetic atoms on metallic surfaces [11].

2. Model of a lateral quantum dot system

The Hamiltonian of interacting electrons confined to a quantum dot has the following general form:

$$H_{\rm dot} = \sum_{s} \sum_{ij} h_{ij} d_{is}^{\dagger} d_{js} + \tfrac{1}{2} \sum_{ss'} \sum_{ijkl} h_{ijkl} d_{is}^{\dagger} d_{js'}^{\dagger} d_{ks'} d_{ls}. \tag{2.1}$$

Here an operator $d_{is}^{\dagger}$ creates an electron with spin s in the orbital state $\phi_i(\boldsymbol{r})$; $h_{ij} = h_{ji}^{*}$ is a Hermitian matrix describing the single-particle part of the Hamiltonian. The matrix elements h_{ijkl} depend on the potential $U(\boldsymbol{r} - \boldsymbol{r}')$ of electron–electron interaction,

$$h_{ijkl} = \int \mathrm{d}\boldsymbol{r}\, \mathrm{d}\boldsymbol{r}'\, \phi_i^{*}(\boldsymbol{r}) \phi_j^{*}(\boldsymbol{r}') U(\boldsymbol{r} - \boldsymbol{r}') \phi_k(\boldsymbol{r}') \phi_l(\boldsymbol{r}). \tag{2.2}$$

The Hamiltonian (2.1) can be simplified further provided that the quasiparticle spectrum is not degenerate near the Fermi level, that the Fermi-liquid theory is applicable to the description of the dot, and that the dot is in the metallic conduction regime. The first of these conditions is satisfied if the dot has no spatial symmetries, which also implies that motion of quasiparticles within the dot is chaotic.

The second condition is met if the electron–electron interaction within the dot is not too strong, i.e. the gas parameter r_s is small,

$$r_s = (k_{\rm F} a_0)^{-1} \lesssim 1, \qquad a_0 = \kappa \hbar^2 / e^2 m^{*}. \tag{2.3}$$

Here k_F is the Fermi wavevector, a_0 is the effective Bohr radius, κ is the dielectric constant of the material, and m^* is the quasiparticle effective mass.

The third condition requires the ratio of the Thouless energy E_T to the mean single-particle level spacing δE to be large [12],

$$g = E_T/\delta E \gg 1. \tag{2.4}$$

For a ballistic two-dimensional dot of linear size L the Thouless energy E_T is of the order of $\hbar v_F/L$, whereas the level spacing can be estimated as

$$\delta E \sim \hbar v_F k_F/N \sim \hbar^2/m^* L^2. \tag{2.5}$$

Here v_F is the Fermi velocity and $N \sim (k_F L)^2$ is the number of electrons in the dot. Therefore,

$$g \sim k_F L \sim \sqrt{N},$$

so that having a large number of electrons $N \gg 1$ in the dot guarantees that condition (2.4) is satisfied.

Under conditions (2.3) and (2.4) the *random matrix theory* (see [13, 14] for a review) is a good starting point for description of non-interacting quasiparticles within the energy strip of width E_T about the Fermi level [12]. The matrix elements h_{ij} in equation (2.1) belong to a Gaussian ensemble [14]. Since the matrix elements do not depend on spin, each eigenvalue ϵ_n of the matrix h_{ij} represents a spin-degenerate energy level. The spacings $\epsilon_{n+1}-\epsilon_n$ between consecutive levels obey the Wigner–Dyson statistics [14]; the mean level spacing $\overline{\epsilon_{n+1}-\epsilon_n} = \delta E$.

We now discuss the second term in Hamiltonian (2.1), which describes electron–electron interaction. It turns out [15–17] that the vast majority of the matrix elements h_{ijkl} are small. Indeed, in the lowest order in $1/g \ll 1$, the wavefunctions $\phi_i(\boldsymbol{r})$ are Gaussian random variables statistically independent of each other and of the corresponding energy levels [18]:

$$\overline{\phi_i^*(\boldsymbol{r})\phi_j(\boldsymbol{r}')} = \frac{1}{L^2}\delta_{ij}F(|\boldsymbol{r}-\boldsymbol{r}'|), \qquad F(r) \sim \langle \exp(\mathrm{i}\boldsymbol{k}\cdot\boldsymbol{r})\rangle_{FS}. \tag{2.6}$$

Here $\langle\cdots\rangle_{FS}$ stands for the averaging over the Fermi surface $|\boldsymbol{k}| = k_F$. In two dimensions, the function $F(r)$ decreases with r as $F \propto (k_F r)^{-1/2}$ at $k_F r \gg 1$, and saturates to $F \sim 1$ at $k_F r \ll 1$. After averaging with the help of equation (2.6), the matrix elements (2.2) take the form[3]

$$\overline{h_{ijkl}} = 2E_C\delta_{il}\delta_{jk} + E_S\delta_{ik}\delta_{jl}.$$

We substitute this expression into Hamiltonian (2.1), and rearrange the sum over the spin indices with the help of the identity

$$2\delta_{s_1s_2}\delta_{s_1's_2'} = \delta_{s_1s_1'}\delta_{s_2s_2'} + \boldsymbol{\sigma}_{s_1s_1'}\cdot\boldsymbol{\sigma}_{s_2s_2'}, \tag{2.7}$$

where $\boldsymbol{\sigma} = (\sigma^x, \sigma^y, \sigma^z)$ are the Pauli matrices. This results in a remarkably simple form [16, 17]

$$H_{int} = E_C\hat{N}^2 - E_S\hat{\mathbf{S}}^2 \tag{2.8}$$

of the interaction part of the Hamiltonian of the dot. Here

$$\hat{N} = \sum_{ns} d_{ns}^\dagger d_{ns}, \qquad \hat{\mathbf{S}} = \sum_{nss'} d_{ns}^\dagger \frac{\boldsymbol{\sigma}_{ss'}}{2} d_{ns'} \tag{2.9}$$

are the operators of the total number of electrons in the dot and of the dot's spin, respectively.

[3] For simplicity we assumed here that $\overline{\phi_i(\boldsymbol{r})\phi_j(\boldsymbol{r}')} \equiv 0$, which corresponds to broken time-reversal symmetry. See [17] for discussion of the general case.

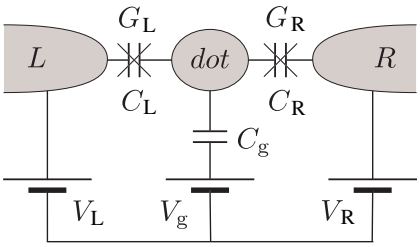

Figure 1. Equivalent circuit for a quantum dot connected to two leads by tunnelling junctions and coupled via a capacitor (with capacitance C_g) to the gate. The total capacitance of the dot $C = C_L + C_R + C_g$.

The first term in equation (2.8) represents the electrostatic energy. In the conventional equivalent circuit picture, see figure 1, the charging energy E_C is related to the total capacitance C of the dot, $E_C = e^2/2C$. For a mesoscopic ($k_F L \gg 1$) conductor, the charging energy is large compared to the mean level spacing δE. Indeed, using the estimates $C \sim \kappa L$ and (2.5), we find

$$E_C/\delta E \sim L/a_0 \sim r_s\sqrt{N}. \tag{2.10}$$

Except for an exotic case of an extremely weak interaction, this ratio is large for $N \gg 1$; for the smallest quantum dots formed in GaAs heterostructures, $E_C/\delta E \sim 10$ [3].

The second term in equation (2.8) describes the intradot exchange interaction, with the exchange energy E_S given by

$$E_S = \int \mathrm{d}\boldsymbol{r}\,\mathrm{d}\boldsymbol{r}'\,U(\boldsymbol{r}-\boldsymbol{r}')F^2(|\boldsymbol{r}-\boldsymbol{r}'|). \tag{2.11}$$

In the case of a long-range interaction the potential U here should properly account for the screening [17]. For $r_s \ll 1$ the exchange energy can be estimated with logarithmic accuracy by substituting $U(r) = (e^2/\kappa r)\theta(a_0 - r)$ into equation (2.11) (here we took into account that the screening length in two dimensions coincides with the Bohr radius a_0), which yields

$$E_S \sim r_s \ln(1/r_s)\delta E \ll \delta E. \tag{2.12}$$

Estimate (2.12) is valid only for $r_s \ll 1$. However, the ratio $E_S/\delta E$ remains small for experimentally relevant[4] values $r_s \sim 1$ as long as the Stoner criterion for the absence of itinerant magnetism [19] is satisfied. This guarantees the absence of a macroscopic (proportional to N) magnetization of a dot in the ground state [16].

Obviously, the interaction part of the Hamiltonian, equation (2.8), is invariant with respect to a change of the basis of single-particle states $\phi_i(\boldsymbol{r})$. Picking up the basis in which the first term in (2.1) is diagonal, we arrive at the *universal Hamiltonian* [16, 17],

$$H_{\mathrm{dot}} = \sum_{ns} \epsilon_n d_{ns}^{\dagger} d_{ns} + E_C\big(\hat{N} - N_0\big)^2 - E_S\hat{\mathbf{S}}^2. \tag{2.13}$$

We included in equation (2.13) the effect of the capacitive coupling to the gate electrode: the dimensionless parameter N_0 is proportional to the gate voltage, $N_0 = C_g V_g/e$, where C_g is the capacitance between the dot and the gate; see figure 1. The relative magnitude of various terms not included in (2.13), as well as that of mesoscopic fluctuations of the coupling constants E_C and E_S, is of the order of $1/g \sim N^{-1/2} \ll 1$.

[4] For GaAs ($m^* \approx 0.07\,m_e$, $\kappa \approx 13$) the effective Bohr radius $a_0 \approx 10$ nm, whereas a typical density of the two-dimensional electron gas, $n \sim 10^{11}$ cm^{-2} [3], corresponds to $k_F = \sqrt{2\pi n} \sim 10^6$ cm^{-1}. This gives $k_F a_0 \sim 1$.

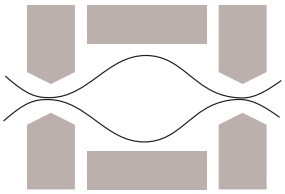

Figure 2. The confining potential forming a lateral quantum dot varies smoothly on the scale of the de Broglie wavelength at the Fermi energy. Hence, the dot–lead junctions act essentially as electronic waveguides with a well defined number of propagating modes.

As discussed above, in this limit the energy scales involved in (2.13) form a well defined hierarchy

$$E_S \ll \delta E \ll E_C. \tag{2.14}$$

If all the single-particle energy levels ϵ_n were equidistant, then the spin S of an even-N state would be zero, while an odd-N state would have $S = 1/2$. However, the level spacings are random. If the spacing between the highest occupied level and the lowest unoccupied one is accidentally small, than the gain in the exchange energy, associated with the formation of a higher-spin state, may be sufficient to overcome the loss of the kinetic energy (cf the Hund rule in quantum mechanics). For $E_S \ll \delta E$ such deviations from the simple even–odd periodicity are rare [16, 20, 21]. This is why the last term in (2.13) is often neglected. Equation (2.13) then reduces to the Hamiltonian of the *constant interaction model*, widely used in the analysis of experimental data [1].

Electron transport through the dot occurs via two dot–lead junctions. In a typical geometry, the potential forming a lateral quantum dot varies smoothly on the scale of the Fermi wavelength; see figure 2. Hence, the point contacts connecting the quantum dot to the leads act essentially as electronic waveguides. Potentials on the gates control the waveguide width, and, therefore, the number of electronic modes the waveguide supports: by making the waveguide narrower one pinches the propagating modes off one by one. Each such mode contributes $2e^2/h$ to the conductance of a contact. The Coulomb blockade develops when the conductances of the contacts are small compared to $2e^2/h$, i.e. when the very last propagating mode approaches its pinch-off [22, 23]. Accordingly, in the Coulomb blockade regime each dot–lead junction in a lateral quantum dot system supports only a single electronic mode [24].

As discussed below, for $E_C \gg \delta E$ the characteristic energy scale relevant to the Kondo effect, the Kondo temperature T_K, is small compared to the mean level spacing: $T_K \ll \delta E$. This separation of the energy scales allows us to simplify the problem even further by assuming that the conductances of the dot–lead junctions are small. This assumption will not affect the properties of the system in the Kondo regime. At the same time, it justifies the use of the tunnelling Hamiltonian for description of the coupling between the dot and the leads. The microscopic Hamiltonian of the system can then be written as a sum of three distinct terms,

$$H = H_{\text{leads}} + H_{\text{dot}} + H_{\text{tunnelling}}, \tag{2.15}$$

which describe free electrons in the leads, the isolated quantum dot, and tunnelling between the dot and the leads, respectively. The second term in (2.15), the Hamiltonian of the dot H_{dot}, is given by equation (2.13). We treat the leads as reservoirs of free electrons with continuous spectra ξ_k, characterized by constant density of states ν, same for both leads. Moreover, since the typical energies $\omega \lesssim E_C$ of electrons participating in transport through a quantum dot in the Coulomb blockade regime are small compared to the Fermi energy of the electron gas in the leads, the spectra ξ_k can be linearized near the Fermi level, $\xi_k = v_F k$; here k is measured

from k_F. With only one electronic mode per junction taken into account, the first and the third terms in equation (2.15) have the form

$$H_{\text{leads}} = \sum_{\alpha k s} \xi_k c^\dagger_{\alpha k s} c_{\alpha k s}, \qquad \xi_k = -\xi_{-k}, \tag{2.16}$$

$$H_{\text{tunnelling}} = \sum_{\alpha k n s} t_{\alpha n} c^\dagger_{\alpha k s} d_{n s} + \text{H.c.} \tag{2.17}$$

Here $t_{\alpha n}$ are tunnelling matrix elements (tunnelling amplitudes) 'connecting' state n in the dot with state k in lead α ($\alpha = \text{R, L}$ for the right/left lead). The randomness of states n translates into the randomness of the tunnelling amplitudes. Indeed, the amplitudes depend on the values of the electron wavefunctions at points $\boldsymbol{r}_\alpha$ of the contacts, $t_{\alpha n} \propto \phi_n(\boldsymbol{r}_\alpha)$. For $k_F L \gg 1$ the wavefunctions are Gaussian random variables. Equation (2.6) then results in

$$\overline{t^*_{\alpha n} t_{\alpha' n'}} = \overline{|t^2_{\alpha n}|}\delta_{\alpha\alpha'}\delta_{nn'}. \tag{2.18}$$

Average values of the tunnelling probabilities can be expressed via the conductances of the dot–lead junctions G_α,

$$\frac{h}{2e^2} G_\alpha = \frac{\Gamma_\alpha}{\delta E} \sim \frac{\nu \overline{|t^2_{\alpha n}|}}{\delta E}. \tag{2.19}$$

Here Γ_α is the rate for an electron to escape from a discrete level n in the dot into lead α.

3. Rate equations and conductance across the dot

At high temperatures, $T \gg E_C$, charging energy is negligible compared to the thermal energy of electrons. Therefore the conductance of the device in this regime G_∞ is not affected by charging and, independently of the gate voltage,

$$\frac{1}{G_\infty} = \frac{1}{G_L} + \frac{1}{G_R}. \tag{3.1}$$

Dependence on N_0 develops at lower temperatures,

$$\delta E \ll T \ll E_C. \tag{3.2}$$

The conductance is not suppressed only within narrow regions—*Coulomb blockade peaks*, i.e. when the gate voltage is tuned sufficiently close to one of the points of charge degeneracy,

$$|N_0 - N_0^*| \lesssim T/E_C; \tag{3.3}$$

here N_0^* is a half-integer number.

We will demonstrate this now using the method of rate equations [25]. In addition to constraint (3.2), we will assume that the inelastic electron relaxation rate within the dot is large compared to the escape rates Γ_α. In other words, transitions between discrete levels in the dot occur before the electron escapes to the leads[5]. Under this assumption the tunnellings across the two junctions can be treated independently of each other. Condition (3.3), on the other hand, allows us to take into account only two charge states of the dot which are almost degenerate in the vicinity of the Coulomb blockade peak. For N_0 close to N_0^* these are the states with $N = N_0^* \pm 1/2$ electrons on the dot. Hereafter we denote these states as $|N\rangle$ and $|N+1\rangle$. Finally, condition (3.2) enables us to replace the discrete single-particle levels within the dot by a continuum with the density of states $1/\delta E$.

[5] Note that a finite inelastic relaxation rate requires inclusion of mechanisms beyond the model (2.13), e.g., electron–phonon collisions.

Applying the Fermi golden rule and using the described simplifications, we may write the current I_α from the lead α into the dot as

$$I_\alpha = \frac{2\pi}{\hbar}\sum_{kns}|t_{\alpha n}|^2\delta(\xi_k + eV_\alpha + E_N - \epsilon_n - E_{N+1}) \times \{P_N f(\xi_k)[1 - f(\epsilon_n)] - P_{N+1} f(\epsilon_n)[1 - f(\xi_k)]\}.$$

Here $f(\omega) = [\exp(\omega/T) + 1]^{-1}$ is the Fermi function, V_α is the potential on lead α (see figure 1), E_N and E_{N+1} are the electrostatic energies of charge states $|N\rangle$ and $|N+1\rangle$, and P_N and P_{N+1} are the probabilities of finding the dot in these states. Replacing the summations over n and k by integrations over the corresponding continua, we find

$$I_\alpha = \frac{G_\alpha}{e}[P_N F(E_1 - E_0 - eV_\alpha) - P_{N+1} F(E_0 - E_1 + eV_\alpha)] \tag{3.4}$$

with $F(\omega) = \omega/[\exp(\omega/T) - 1]$. In equilibrium, the current (3.4) is zero by the detailed balance. When a finite current flows through the junction the probabilities P_N and P_{N+1} deviate from their equilibrium values. In the steady state, the currents across the two junctions satisfy

$$I = I_{\mathrm{L}} = -I_{\mathrm{R}}. \tag{3.5}$$

Equations (3.4) and (3.5), supplemented by the obvious normalization condition $P_N + P_{N+1} = 1$, allow one to find P_N, P_{N+1}, and the current across the dot I in response to the applied bias $V = V_{\mathrm{L}} - V_{\mathrm{R}}$. The linear conductance across the dot $G = \lim_{V\to 0} \mathrm{d}I/\mathrm{d}V$ is then given by [25]

$$G = G_\infty \frac{E_{\mathrm{C}}(N_0 - N_0^*)/T}{\sinh[2E_{\mathrm{C}}(N_0 - N_0^*)/T]}. \tag{3.6}$$

Here $N_0 - N_0^* = 0$ (half-integer N_0) corresponds to the Coulomb blockade peak. In the *Coulomb blockade valleys* ($N_0 \neq N_0^*$), conductance falls off exponentially with the decrease of temperature, and all the valleys behave exactly the same way.

4. Activationless transport through a blockaded quantum dot

According to the rate equation theory [25], at low temperatures, $T \ll E_{\mathrm{C}}$, conduction through the dot is exponentially suppressed in the Coulomb blockade valleys. This suppression occurs because the process of electron transport through the dot involves a *real transition* to the state in which the charge of the dot differs by e from the thermodynamically most probable value. The probability of such fluctuation is proportional to $\exp(-E_{\mathrm{C}}|N_0 - N_0^*|/T)$, which explains the conductance suppression; see equation (3.5). Going beyond the lowest-order perturbation theory in conductances G_α allows one to consider processes in which states of the dot with a 'wrong' charge participate in the tunnelling process as *virtual states*. The existence of these higher-order contributions to the tunnelling conductance was envisioned first by Giaever and Zeller [26]. The first quantitative theory of this effect, however, was developed much later [27].

The leading contributions to the activationless transport, according to [27], are provided by the processes of *inelastic and elastic co-tunnelling*. Unlike the sequential tunnelling, in the co-tunnelling mechanism, the events of electron tunnelling from one of the leads into the dot, and tunnelling from the dot to the other lead occur as a single quantum process.

4.1. Inelastic co-tunnelling

In the inelastic co-tunnelling mechanism, an electron tunnels from a lead into one of the vacant single-particle levels in the dot, while it is an electron occupying some other level that tunnels

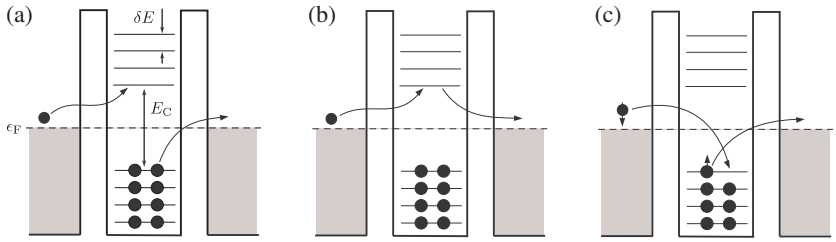

Figure 3. Examples of the co-tunnelling processes. (a) Inelastic co-tunnelling: transferring of an electron between the leads leaves behind an electron–hole pair in the dot; (b) elastic co-tunnelling; (c) elastic co-tunnelling with a flip of spin.

out of the dot; see figure 3(a). As a result, transfer of charge e between the leads is accompanied by a simultaneous creation of an electron–hole pair in the dot.

Here we will estimate the contribution of the inelastic co-tunnelling to the conductance deep in the Coulomb blockade valley, i.e. at almost integer N_0. Consider an electron that tunnels into the dot from lead L. If energy ω of the electron relative to the Fermi level is small compared to the charging energy, $\omega \ll E_C$, then the energy of the virtual state involved in the co-tunnelling process is close to E_C. The amplitude A_{in} of the inelastic transition via this virtual state to lead R is then given by

$$A_{in} = \frac{t^*_{Ln}\, t_{Rn'}}{E_C}. \tag{4.1}$$

The initial state of this transition has an extra electron in the single-particle state k in lead L, while the final state has an extra electron in state k' in lead R and an electron–hole pair in the dot (state n is occupied; state n' is empty).

Given the energy of the initial state ω, the number of available final states can be estimated from the phase space argument, familiar from the calculation of the quasiparticle lifetime in the Fermi liquid theory [28]. For $\omega \gg \delta E$ this number is of the order of $(\omega/\delta E)^2$. Since the typical value of ω is T, the inelastic co-tunnelling contribution to the conductance can be estimated as

$$G_{in} \sim \frac{e^2}{h}\left(\frac{T}{\delta E}\right)^2 \nu^2 \overline{|A^2_{in}|}.$$

Now using equations (2.18) and (2.19), we find [27]

$$G_{in} \sim \frac{h}{e^2}\, G_L G_R \left(\frac{T}{E_C}\right)^2. \tag{4.2}$$

A comparison of equation (4.2) with the result of the rate equation theory (3.6) shows that the inelastic co-tunnelling takes over the thermally activated hopping at moderately low temperatures

$$T \lesssim T_{in} = E_C \left[\ln\left(\frac{e^2/h}{G_L + G_R}\right)\right]^{-1}. \tag{4.3}$$

The smallest energy of the electron–hole pair is of the order of δE. At temperatures below this threshold the inelastic co-tunnelling contribution to the conductance becomes exponentially small. It turns out, however, that even at much higher temperatures this mechanism becomes less effective than the elastic co-tunnelling.

4.2. Elastic co-tunnelling

In the process of elastic co-tunnelling, transfer of charge between the leads is not accompanied by the creation of an electron–hole pair in the dot. In other words, occupation numbers of single-particle energy levels in the dot in the initial and final states of the co-tunnelling process are exactly the same; see figure 3(b). Close to the middle of the Coulomb blockade valley (at almost integer N_0) the average number of electrons on the dot, $N \approx N_0$, is also an integer. Both an addition and a removal of a single electron cost E_C in electrostatic energy; see equation (2.13). The amplitude of the elastic co-tunnelling process in which an electron is transferred from lead L to lead R can then be written as

$$A_{el} = \sum_n A_n, \qquad A_n = t^*_{Ln} t_{Rn} \frac{\theta(\epsilon_n) - \theta(-\epsilon_n)}{E_C + |\epsilon_n|}. \tag{4.4}$$

The two contributions to the partial amplitude A_n are associated with virtual creation of either an electron if level n is empty ($\epsilon_n > 0$), or of a hole if the level is occupied ($\epsilon_n < 0$); the relative sign difference between the two contributions originates in the fermionic commutation relations.

With the help of equations (2.18) and (2.19) the average value of the elastic co-tunnelling contribution to the conductance can be written as

$$\overline{G_{el}} = \frac{2e^2}{h} \nu^2 \overline{|A^2_{el}|} \sim \frac{h}{e^2} G_L G_R \sum_n \left(\frac{\delta E}{E_C + |\epsilon_n|} \right)^2.$$

Since for $E_C \gg \delta E$ the number of terms making significant contributions to the sum over n here is large, and since the sum is converging, one can replace the summation by an integral which results in [27]

$$\overline{G_{el}} \sim \frac{h}{e^2} G_L G_R \frac{\delta E}{E_C}. \tag{4.5}$$

Comparison with equation (4.2) shows that the elastic co-tunnelling dominates the electron transport already at temperatures

$$T \lesssim T_{el} = \sqrt{E_C \delta E}, \tag{4.6}$$

which may significantly exceed the level spacing. Note, however, that mesoscopic fluctuations of G_{el} are strong [29], of the order of its average value (4.5). Thus, although $\overline{G_{el}}$ is always positive (see equation (4.6)), the sample-specific value of G_{el} for a given gate voltage may vanish [30].

5. Effective low-energy Hamiltonian

In the above discussion of the elastic co-tunnelling we made a tacit assumption that all single-particle levels in the dot are either empty or doubly occupied. This, however, is not the case when the dot has a non-zero spin in the ground state. A dot with an odd number of electrons, for example, would necessarily have a half-integer spin S. In the most important case of $S = 1/2$ the top-most occupied single-particle level is filled by a single electron and is spin degenerate. This opens a possibility of a co-tunnelling process in which a transfer of an electron between the leads is accompanied by a flip of the electron's spin with simultaneous flip of the spin on the dot; see figure 3(c).

The amplitude of such a process, calculated in the fourth order in tunnelling matrix elements, diverges logarithmically when the energy ω of an incoming electron approaches zero. Since $\omega \sim T$, the logarithmic singularity in the transmission amplitude translates into

a dramatic enhancement of the conductance G across the dot at low temperatures: G may reach values as high as the quantum limit $2e^2/h$ [31, 32]. This conductance enhancement is not really a surprise. Indeed, in the spin-flip co-tunnelling process a quantum dot with odd N behaves as an $S = 1/2$ magnetic impurity embedded in a tunnelling barrier separating two massive conductors [33]. It has been known [34] since the mid-1960s that the presence of such impurities leads to zero-bias anomalies in tunnelling conductance [35], which are adequately explained [36, 37] in the context of the Kondo effect [5].

At energies well below the threshold $\Delta \sim \delta E$ for intradot excitations the transitions within the $(2S + 1)$-fold degenerate ground state manifold of a dot can be conveniently described by a spin operator $\mathbf{S}$. The form of the *effective Hamiltonian* describing the interaction of the dot with conduction electrons in the leads is then dictated by $SU(2)$ symmetry[6],

$$H_{\text{eff}} = \sum_{\alpha k s} \xi_k \, c^{\dagger}_{\alpha k s} c_{\alpha k s} + \sum_{\alpha\alpha'} J_{\alpha\alpha'} (\mathbf{s}_{\alpha'\alpha} \cdot \mathbf{S}) \tag{5.1}$$

with $\mathbf{s}_{\alpha\alpha'} = \sum_{k k' s s'} c^{\dagger}_{\alpha k s} (\boldsymbol{\sigma}_{s s'}/2)\, c_{\alpha' k' s'}$. The sum over k in equation (5.1) is restricted to $|\xi_k| < \Delta$. The exchange amplitudes $J_{\alpha\alpha'}$ form a 2×2 Hermitian matrix $\hat{J}$. The matrix has two real eigenvalues, the exchange constants J_1 and J_2 (hereafter we assume that $J_1 \geqslant J_2$). By an appropriate rotation in the R–L space the Hamiltonian (5.2) can then be brought into the form

$$H_{\text{eff}} = \sum_{\gamma k s} \xi_k \, \psi^{\dagger}_{\gamma k s} \psi_{\gamma k s} + \sum_{\gamma} J_{\gamma} (\mathbf{s}_{\gamma} \cdot \mathbf{S}). \tag{5.2}$$

Here the operators ψ_γ are certain linear combinations of the original operators $c_{\text{R,L}}$ describing electrons in the leads, and

$$\mathbf{s}_{\gamma} = \sum_{k k' s s'} \psi^{\dagger}_{\gamma k s} \frac{\boldsymbol{\sigma}_{s s'}}{2} \psi_{\gamma k' s'}$$

is the local spin density of itinerant electrons in the 'channel' $\gamma = 1, 2$.

The symmetry alone is not sufficient to determine the exchange constants J_γ; their evaluation must rely upon a microscopic model. Here we briefly outline the derivation [24, 38] of equation (5.1) for a generic model of a quantum dot system discussed in section 2 above. For simplicity, we will assume that the gate voltage N_0 is tuned to the middle of the Coulomb blockade valley. The tunnelling (2.17) mixes the state with $N = N_0$ electrons on the dot with states having $N \pm 1$ electrons. The electrostatic energies of these states are high ($\sim E_{\text{C}}$), hence the transitions $N \to N \pm 1$ are virtual, and can be taken into account perturbatively in the second order in tunnelling amplitudes [39].

For Hamiltonian (2.13) the occupations of single-particle energy levels are good quantum numbers. Therefore, the amplitude $J_{\alpha\alpha'}$ can be written as a sum of partial amplitudes,

$$J_{\alpha\alpha'} = \sum_{n} J^{n}_{\alpha\alpha'}. \tag{5.3}$$

Each term in the sum here corresponds to a process during which an electron or a hole is created virtually on level n in the dot, cf equation (4.4). For $G_\alpha \ll e^2/h$ and $E_{\text{S}} \ll \delta E$ the main contribution to the sum in (5.3) comes from singly occupied energy levels in the dot. A dot with spin S has $2S$ such levels near the Fermi level (hereafter we assign indices $n = -S, \ldots, n = S$ to these levels), each carrying a spin $\mathbf{S}/2S$, and contributing

$$J^{n}_{\alpha\alpha'} = \frac{\lambda_n}{E_{\text{C}}} t^{*}_{\alpha n} t_{\alpha' n}, \qquad \lambda_n = 2/S, \quad |n| \leqslant S \tag{5.4}$$

[6] In writing equation (5.1) we omitted the potential scattering terms associated with the usual elastic co-tunnelling. This approximation is well justified when the conductances of the dot–lead junctions are small, $G_\alpha \ll e^2/h$, in which case G_{el} is also very small; see equation (4.5).

to the exchange amplitude in (5.1). This yields

$$J_{\alpha\alpha'} \approx \sum_{|n|\leqslant S} J^n_{\alpha\alpha'}. \tag{5.5}$$

It follows from equations (5.3) and (5.4) that

$$\operatorname{tr} \hat{J} = \frac{1}{E_{\mathrm{C}}} \sum_n \lambda_n \left(|t^2_{\mathrm{L}n}| + |t^2_{\mathrm{R}n}| \right). \tag{5.6}$$

By restricting the sum over n here to $|n| \leqslant S$, as in (5.5), and taking into account that all λ_n in (5.4) are positive, we find $J_1 + J_2 > 0$. Similarly, from

$$\det \hat{J} = \frac{1}{2E^2_{\mathrm{C}}} \sum_{m,n} \lambda_m \lambda_n |\mathcal{D}^2_{mn}|, \qquad \mathcal{D}_{mn} = \det \begin{pmatrix} t_{\mathrm{L}m} & t_{\mathrm{R}m} \\ t_{\mathrm{L}n} & t_{\mathrm{R}n} \end{pmatrix} \tag{5.7}$$

and equations (5.4) and (5.5) it follows that $J_1 J_2 > 0$ for $S > 1/2$. Indeed, in this case the sum in (5.7) contains at least one contribution with $m \neq n$; all such contributions are positive. Thus, both exchange constants $J_{1,2} > 0$ if the dot's spin S exceeds $1/2$ [24]. The pecularities of the Kondo effect in quantum dots with large spin are discussed in section 7 below.

Here we concentrate on the most common situation of $S = 1/2$ on the dot [3], considered in detail in section 6. The ground state of such a dot has only one singly occupied energy level ($n = 0$), so that $\det \hat{J} \approx 0$; see (5.5) and (5.7). Accordingly, one of the exchange constants vanishes,

$$J_2 \approx 0, \tag{5.8}$$

while the remaining one, $J_1 = \operatorname{tr} \hat{J}$, is positive. Equation (5.8) resulted, of course, from the approximation made in (5.5). For model (2.13) the leading correction to (5.5) originates in the co-tunnelling processes with an intermediate state containing an extra electron (or an extra hole) on one of the empty (doubly occupied) levels. Such a contribution arises because the spin on level n is not conserved by the Hamiltonian (2.13), unlike the corresponding occupation number. Straightforward calculation [38] yields the partial amplitude in the form of (5.4), but with

$$\lambda_n = -\frac{2E_{\mathrm{C}}E_{\mathrm{S}}}{(E_{\mathrm{C}} + |\epsilon_n|)^2}, \qquad n \neq 0.$$

Unless the tunnelling amplitudes $t_{\alpha 0}$ to the only singly occupied level in the dot are anomalously small, the corresponding correction

$$\delta J_{\alpha\alpha'} = \sum_{n\neq 0} J^n_{\alpha\alpha'} \tag{5.9}$$

to the exchange amplitude (5.5) is small,

$$\left| \frac{\delta J_{\alpha\alpha'}}{J_{\alpha\alpha'}} \right| \sim \frac{E_{\mathrm{S}}}{\delta E} \ll 1;$$

see equation (2.14). To obtain this estimate, we assumed that all tunnelling amplitudes $t_{\alpha n}$ are of the same order of magnitude, and replaced the sum over n in (5.9) by an integral. A similar estimate yields the leading contribution to $\det \hat{J}$,

$$\det \hat{J} \approx \frac{1}{E^2_{\mathrm{C}}} \sum_n \lambda_0 \lambda_n |\mathcal{D}^2_{0n}| \sim -\frac{E_{\mathrm{S}}}{\delta E} \left(\operatorname{tr} \hat{J} \right)^2,$$

or

$$J_2/J_1 \sim -E_{\mathrm{S}}/\delta E. \tag{5.10}$$

According to (5.10), the exchange constant J_2 is negative [40], and its absolute value is small compared to J_1. Hence, (5.8) is indeed an excellent approximation for large chaotic dots with spin $S = 1/2$ as long as the intradot exchange interaction remains weak, $E_S \ll \delta E$.[7] Note that corrections to the universal Hamiltonian (2.13) also result in finite values of both exchange constants, $|J_2| \sim J_1 N^{-1/2}$, and become important for small dots with $N \lesssim 10$ [32]. Although this may significantly affect the conductance across the system in the weak-coupling regime $T \gtrsim T_K$, it does not lead to qualitative changes in the results for $S = 1/2$ on the dot, as the channel with smaller exchange constant decouples at low energies [42]; see also section 7 below. With this caveat, we adopt approximation (5.8) in our description of the Kondo effect in quantum dots with spin $S = 1/2$. Accordingly, the effective Hamiltonian of the system (5.2) assumes the 'block-diagonal' form

$$H_{\rm eff} = H_1 + H_2 \tag{5.11}$$

$$H_1 = \sum_{ks} \xi_k \psi^\dagger_{1ks} \psi_{1ks} + J(\mathbf{s}_1 \cdot \mathbf{S}) \tag{5.12}$$

$$H_2 = \sum_{ks} \xi_k \psi^\dagger_{2ks} \psi_{2ks} \tag{5.13}$$

with $J = \operatorname{tr} \hat{J} > 0$.

6. Kondo regime in transport through a quantum dot

To get an idea about the physics of the Kondo model (see [43] for recent reviews), let us first replace the fermion field operator $\mathbf{s}_1$ in equation (5.12) by a single-particle spin-1/2 operator $\mathbf{S}_1$. The ground state of the resulting Hamiltonian of two spins

$$\tilde{H} = J(\mathbf{S}_1 \cdot \mathbf{S})$$

is obviously a singlet. The excited state (a triplet) is separated from the ground state by the energy gap J_1. This separation can be interpreted as the binding energy of the singlet. Unlike $\mathbf{S}_1$ in this simple example, the operator $\mathbf{s}_1$ in (5.12) is merely a spin density of the conduction electrons at the site of the 'magnetic impurity'. Because conduction electrons are freely moving in space, it is hard for the impurity to 'capture' an electron and form a singlet. Yet, even a weak local exchange interaction suffices to form a singlet ground state [44, 45]. However, the characteristic energy (an analogue of the binding energy) for this singlet is given not by the exchange constant J, but by the so-called Kondo temperature

$$T_K \sim \Delta \exp(-1/\nu J). \tag{6.1}$$

Using $\Delta \sim \delta E$ and equations (5.6) and (2.19), one obtains from (6.1) the estimate

$$\ln\left(\frac{\delta E}{T_K}\right) \sim \frac{1}{\nu J} \sim \frac{e^2/h}{G_L + G_R} \frac{E_C}{\delta E}. \tag{6.2}$$

Since $G_\alpha \ll e^2/h$ and $E_C \gg \delta E$, the rhs of (6.2) is a product of two large parameters. Therefore, the Kondo temperature T_K is small compared to the mean level spacing,

$$T_K \ll \delta E. \tag{6.3}$$

It is this separation of the energy scales that justifies the use of the effective low-energy Hamiltonian (5.1), (5.2) for the description of the Kondo effect in a quantum dot system.

[7] Equation (5.8) holds identically for the Anderson impurity model [37] frequently employed to study transport through quantum dots [31, 41]. In that model a quantum dot is described by a single energy level, which formally corresponds to the infinite level spacing limit $\delta E \to \infty$ of the Hamiltonian (2.13).

Inequality (6.3) remains valid even if the conductances of the dot–lead junctions G_α are of the order of $2e^2/h$. However, in this case estimate (6.2) is no longer applicable [46].

In our model, see equations (5.11)–(5.13), one of the channels (ψ_2) of conduction electrons completely decouples from the dot, while the ψ_1 particles are described by the standard single-channel antiferromagnetic Kondo model [5, 43]. Therefore, the thermodynamic properties of a quantum dot in the Kondo regime are identical to those of the conventional Kondo problem for a single magnetic impurity in a bulk metal; thermodynamics of the latter model is fully studied [47]. However, all the experiments addressing the Kondo effect in quantum dots test their transport properties rather than thermodynamics. The electron current operator is not diagonal in the (ψ_1, ψ_2) representation, and the contributions of these two sub-systems to the conductance are not additive. Below we relate the linear conductance and, in some special case, the non-linear differential conductance as well, to the t-matrix of the conventional Kondo problem.

6.1. Linear response

The linear conductance can be calculated from the Kubo formula

$$G = \lim_{\omega\to 0} \frac{1}{\hbar\,\omega} \int_0^\infty \mathrm{d}t\, \mathrm{e}^{\mathrm{i}\omega t} \left\langle \left[\hat{I}(t), \hat{I}(0)\right]\right\rangle, \tag{6.4}$$

where the current operator $\hat{I}$ is given by

$$\hat{I} = \frac{\mathrm{d}}{\mathrm{d}t}\frac{e}{2}\left(\hat{N}_\mathrm{R} - \hat{N}_\mathrm{L}\right), \qquad \hat{N}_\alpha = \sum_{ks} c^\dagger_{\alpha ks} c_{\alpha ks}. \tag{6.5}$$

Here $\hat{N}_\alpha$ is the operator of the total number of electrons in lead α. Evaluation of the linear conductance proceeds similarly to the calculation of the impurity contribution to the resistivity of dilute magnetic alloys (see, e.g., [48]). In order to take the full advantage of the decomposition (5.11)–(5.13), we rewrite $\hat{I}$ in terms of the operators $\psi_{1,2}$. These operators are related to the original operators $c_{\mathrm{R,L}}$ representing the electrons in the right- and left-hand leads via

$$\begin{pmatrix} \psi_{1ks} \\ \psi_{2ks} \end{pmatrix} = \begin{pmatrix} \cos\theta_0 & \sin\theta_0 \\ -\sin\theta_0 & \cos\theta_0 \end{pmatrix} \begin{pmatrix} c_{\mathrm{R}ks} \\ c_{\mathrm{L}ks} \end{pmatrix}. \tag{6.6}$$

The rotation matrix here is the same one that diagonalizes matrix $\hat{J}$ of the exchange amplitudes in (5.1); the rotation angle θ_0 satisfies the equation $\tan\theta_0 = |t_{\mathrm{L}0}/t_{\mathrm{R}0}|$. With the help of equation (6.6) we obtain

$$\hat{N}_\mathrm{R} - \hat{N}_\mathrm{L} = \cos(2\theta_0)\left(\hat{N}_1 - \hat{N}_2\right) - \sin(2\theta_0) \sum_{ks} \left(\psi^\dagger_{1ks}\psi_{2ks} + \mathrm{H.c.}\right). \tag{6.7}$$

The current operator $\hat{I}$ entering the Kubo formula (6.4) is to be calculated with the equilibrium Hamiltonian (5.11)–(5.13). Since both $\hat{N}_1$ and $\hat{N}_2$ commute with H_eff, the first term in (6.7) makes no contribution to $\hat{I}$. When the second term in (6.7) is substituted into (6.5) and then into the Kubo formula (6.4), the result, after integration by parts, can be expressed via two-particle correlation functions such as $\left\langle \psi^\dagger_1(t)\psi_2(t)\psi^\dagger_2(0)\psi_1(0)\right\rangle$ (see appendix B of [49] for further details of this calculation). Due to the block-diagonal structure of H_eff (see (5.11)), these correlation functions factorize into products of the single-particle correlation functions describing the (free) ψ_2 particles and the (interacting) ψ_1 particles. The result of the evaluation of the Kubo formula can then be written as

$$G = G_0 \int \mathrm{d}\omega \left(-\frac{\mathrm{d}f}{\mathrm{d}\omega}\right) \frac{1}{2} \sum_s \left[-\pi\nu\,\mathrm{Im}\,T_s(\omega)\right]. \tag{6.8}$$

Here

$$G_0 = \frac{2e^2}{h}\sin^2(2\theta_0) = \frac{2e^2}{h}\frac{4|t_{\mathrm{L}0}^2 t_{\mathrm{R}0}^2|}{\left(|t_{\mathrm{L}0}^2| + |t_{\mathrm{R}0}^2|\right)^2}, \tag{6.9}$$

$f(\omega)$ is the Fermi function, and $T_s(\omega)$ is the t-matrix for the Kondo model (5.12). The t-matrix is related to the exact retarded Green function of the ψ_1 particles in the conventional way,

$$G_{ks,k's}(\omega) = G_k^0(\omega) + G_k^0(\omega)T_s(\omega)G_{k'}^0(\omega), \qquad G_k^0 = (\omega - \xi_k + \mathrm{i}0)^{-1}.$$

Here $G_{ks,k's}(\omega)$ is the Fourier transform of $G_{ks,k's}(t) = -\mathrm{i}\theta(t)\langle\{\psi_{1ks}(t), \psi_{1k's}^{\dagger}\}\rangle$, where $\langle\cdots\rangle$ stands for the thermodynamic averaging with Hamiltonian (5.12). In writing equation (6.8) we took into account the conservation of the total spin (which implies that $G_{ks,k's'} = \delta_{ss'}G_{ks,k's}$, and that the interaction in (5.12) is local (which in turn means that the t-matrix is independent of k and k').

6.2. Weak-coupling regime: $T_K \ll T \ll \delta E$

When the exchange term in Hamiltonian (5.12) is treated perturbatively, the main contribution to the t-matrix comes from the transitions of the type [50]

$$|ks,\sigma\rangle \to \left|k's',\sigma'\right\rangle. \tag{6.10}$$

Here state $|ks,\sigma\rangle$ has an extra electron with spin s in orbital state k whereas the dot is in spin state σ. By $SU(2)$ symmetry, the amplitude of transition (6.10) satisfies

$$A_{|k's',\sigma'\rangle\leftarrow|ks,\sigma\rangle} = A_{k'k}\,\tfrac{1}{4}\left(\boldsymbol{\sigma}_{s's}\cdot\boldsymbol{\sigma}_{\sigma'\sigma}\right). \tag{6.11}$$

Transition (6.10) is *elastic* in the sense that the number of quasiparticles in the final state of the transition is the same as that in the initial state (in other words, transition (6.10) is not accompanied by the production of electron–hole pairs). Therefore, the imaginary part of the t-matrix can be calculated with the help of the optical theorem [51], which yields

$$-\pi\nu\,\mathrm{Im}\,T_s = \tfrac{1}{2}\sum_{\sigma}\sum_{s'\sigma'}\left|\pi\nu A^2_{|k's',\sigma'\rangle\leftarrow|ks,\sigma\rangle}\right|. \tag{6.12}$$

The factor $1/2$ here accounts for the probability of having spin σ on the dot in the initial state of the transition. Substitution of the tunnelling amplitude in the form (6.11) into equation (6.12) and summation over the spin indices with the help of the identity (2.7) result in

$$-\pi\nu\,\mathrm{Im}\,T_s = \frac{3\pi^2}{16}\nu^2\left|A^2_{k'k}\right|. \tag{6.13}$$

The amplitude $A_{k'k}$ in equations (6.11) and (6.13) depends only on the difference of energies $\omega = \xi_{k'} - \xi_k$,

$$A_{k'k} = A(\omega).$$

In the leading (first) order in J one readily obtains $A^{(1)} = J$, independently of ω. However, as discovered by Kondo [5], the second-order contribution $A^{(2)}$ not only depends on ω, but is logarithmically divergent as $\omega \to 0$:

$$A^{(2)}(\omega) = \nu J^2 \ln|\Delta/\omega|.$$

Here Δ is the high-energy cut-off in Hamiltonian (5.12). It turns out [50] that similar logarithmically divergent contributions appear in all orders of perturbation theory,

$$\nu A^{(n)}(\omega) = (\nu J)^n\left[\ln|\Delta/\omega|\right]^{n-1},$$

resulting in a geometric series

$$\nu A(\omega) = \sum_{n=1}^{\infty} \nu A^{(n)} = \nu J \sum_{n=0}^{\infty} \left[\nu J \ln|\Delta/\omega|\right]^n = \frac{\nu J}{1 - \nu J \ln|\Delta/\omega|}.$$

With the help of the definition of the Kondo temperature (6.1), this can be written as

$$\nu A(\omega) = \frac{1}{\ln|\omega/T_K|}. \tag{6.14}$$

Substitution of (6.14) into equation (6.13) and then into equation (6.8), and evaluation of the integral over ω with logarithmic accuracy, yield for the conductance across the dot

$$G = G_0 \frac{3\pi^2/16}{\ln^2(T/T_K)}, \qquad T \gg T_K. \tag{6.15}$$

Equation (6.15) is the leading term of the asymptotic expansion in powers of $1/\ln(T/T_K)$, and represents the conductance in the *leading logarithmic approximation*.

Equation (6.15) resulted from summing up the most-diverging contributions in all orders of perturbation theory. It is instructive to re-derive it now in the framework of the *renormalization group* [52]. The idea of this approach rests on the observation that the electronic states that give a significant contribution to observable quantities, such as conductance, are states within an interval of energies of width $\omega \sim T$ about the Fermi level; see equation (6.8). At temperatures of the order of T_K, when the Kondo effect becomes important, this interval is narrow compared to the width of the band $D = \Delta$ in which the Hamiltonian (5.12) is defined.

Consider a narrow strip of energies of the width $\delta D \ll D$ near the edge of the band. Any transition (6.10) between a state near the Fermi level and one of the states in the strip is associated with high ($\sim\Delta$) energy deficit, and, therefore, can only occur virtually. Obviously, virtual transitions via each of the states in the strip result in the second-order correction $\sim J^2/D$ to the amplitude $A(\omega)$ of the transition between states in the vicinity of the Fermi level. Since the strip contains $\nu\delta D$ electronic states, the total correction is [52]

$$\delta A \sim \nu J^2 \delta D/D.$$

This correction can be accounted for by modifying the exchange constant in the effective Hamiltonian $\tilde{H}_{\rm eff}$ which is defined for states within a narrower energy band of width $D - \delta D$ [52],

$$\tilde{H}_{\rm eff} = \sum_{ks} \xi_k \psi^\dagger_{ks} \psi_{ks} + J_{D-\delta D}(\mathbf{s}_\psi \cdot \mathbf{S}), \qquad |\xi_k| < D - \delta D, \tag{6.16}$$

$$J_{D-\delta D} = J_D + \nu J_D^2 \frac{\delta D}{D}. \tag{6.17}$$

Here J_D is the exchange constant in the original Hamiltonian. Note that $\tilde{H}_{\rm eff}$ has the same form as equation (5.12). This is not merely a conjecture, but can be shown rigorously [45, 53].

The reduction of the bandwidth can be considered to be a result of a unitary transformation that decouples the states near the band edges from the rest of the band. In principle, any such transformation should also affect the operators that describe the observable quantities. Fortunately, this is not the case for the problem at hand. Indeed, angle θ_0 in equation (6.6) is not modified by the transformation. Therefore, the current operator and the expression for the conductance (6.8) retain their form.

Successive reductions of D by small steps δD can be viewed as a continuous process during which the initial Hamiltonian (5.12) with $D = \Delta$ is transformed to an effective Hamiltonian of the same form that acts within the band of the reduced width $D \ll \Delta$. It follows from (6.17)

that the dependence of the effective exchange constant on D is described by the differential equation [52, 53]

$$\frac{\mathrm{d}J_D}{\mathrm{d}\zeta} = \nu J_D^2, \qquad \zeta = \ln(\Delta/D). \tag{6.18}$$

With the help of equation (6.1), the solution of the RG equation (6.18) subject to the initial condition $J_\Delta = J$ can be cast in the form

$$\nu J_D = \frac{1}{\ln(D/T_\mathrm{K})}.$$

The renormalization described by equation (6.18) can be continued until the bandwidth D becomes of the order of the typical energy $|\omega| \sim T$ for real transitions. After this limit has been reached, the transition amplitude $A(\omega)$ is calculated in lowest (first) order of perturbation theory in the effective exchange constant (higher order contributions are negligibly small for $D \sim \omega$),

$$\nu A(\omega) = \nu J_{D\sim|\omega|} = \frac{1}{\ln|\omega/T_\mathrm{K}|}.$$

Now using equations (6.13) and (6.8), we recover equation (6.15).

6.3. Strong-coupling regime: $T \ll T_K$

As temperature approaches T_K, the leading logarithmic approximation result (6.15) diverges. This divergence signals the failure of the approximation. Indeed, we are considering a model with single-mode junctions between the dot and the leads. The maximal possible conductance in this case is $2e^2/h$. To obtain a more precise bound, we discuss in this section the conductance in the strong-coupling regime $T \ll T_\mathrm{K}$.

We start with the zero-temperature limit $T = 0$. As discussed above, the ground state of the Kondo model (5.12) is a singlet [44], and, accordingly, is not degenerate. Therefore, the t-matrix of the conduction electrons interacting with the localized spin is completely characterized by the scattering phase shifts δ_s for electrons with spin s at the Fermi level. The t-matrix is then given by the standard scattering theory expression [51]

$$-\pi\nu T_s(0) = \frac{1}{2\mathrm{i}}\left(\mathbb{S}_s - 1\right), \qquad \mathbb{S}_s = \mathrm{e}^{2\mathrm{i}\delta_s}, \tag{6.19}$$

where $\mathbb{S}_s$ is the scattering matrix for electrons with spin s, which for a single-channel case reduces to its eignevalue. Substitution of (6.19) into equation (6.8) yields

$$G(0) = G_0 \tfrac{1}{2}\sum_s \sin^2\delta_s \tag{6.20}$$

for the conductance; see equation (6.8). The phase shifts in (6.19) and (6.20) are obviously defined only mod π (that is, δ_s and $\delta_s + \pi$ are equivalent). This ambiguity can be removed if we set to zero the values of the phase shifts at $J = 0$ in equation (5.12).

In order to find the two phase shifts δ_s, we need two independent relations. The first one follows from the invariance of the Kondo Hamiltonian (5.12) under the particle–hole transformation $\psi_{ks} \to s\psi^\dagger_{-k,-s}$ (here $s = \pm 1$ for spin-up/down electrons). The particle–hole symmetry implies the relation for the t-matrix

$$T_s(\omega) = -T^*_{-s}(-\omega), \tag{6.21}$$

valid at all ω and T. In view of equation (6.19), it translates into the relation for the phase shifts at the Fermi level ($\omega = 0$) [54],

$$\delta_\uparrow + \delta_\downarrow = 0. \tag{6.22}$$

The second relation follows from the requirement that the ground state of Hamiltonian (5.12) is a singlet [54]. In the absence of exchange ($J = 0$) and at $T = 0$, an infinitesimally weak ($B \to +0$) magnetic field acting on the dot's spin,

$$H_B = BS^z, \tag{6.23}$$

would polarize it; here B is the Zeeman energy. Since a free electron gas has zero spin in the ground state, the total spin in a very large but finite region of space $\mathcal{V}$ surrounding the dot coincides with the spin of the dot, $\langle S^z \rangle_{J=0} = -1/2$. If the exchange with the electron gas is now turned on, $J > 0$, a very weak field will not prevent the formation of a singlet ground state. In this state, the total spin within $\mathcal{V}$ is zero. Such change of the spin is possible if the numbers of spin-up and spin-down electrons within $\mathcal{V}$ have changed to compensate for the dot's spin: $\delta N_\uparrow - \delta N_\downarrow = 1$. By the Friedel sum rule, δN_s are related to the scattering phase shifts at the Fermi level, $\delta N_s = \delta_s/\pi$, which gives

$$\delta_\uparrow - \delta_\downarrow = \pi. \tag{6.24}$$

Combining (6.22) and (6.24), we find $|\delta_s| = \pi/2$. Equation (6.20) then yields for zero-temperature and zero-field conductance across the dot [31]

$$G(0) = G_0. \tag{6.25}$$

Thus, the growth of the conductance with lowering the temperature is limited only by the value of G_0. This value (see equation (6.9)) depends only on the ratio of the tunnelling amplitudes $|t_{L0}/t_{R0}|$. If $|t_{L0}| = |t_{R0}|$, then the conductance at $T = 0$ will reach the maximal value $G = 2e^2/h$ allowed by quantum mechanics [31].

The maximal conductance, equation (6.25), is reached when a singlet state is formed by the itinerant electrons interacting with the local spin, as described by the Kondo Hamiltonian (5.12). Perturbation of this singlet [54] by a magnetic field B or temperature T leads to a decrease of the conductance. This decrease is small as long as B and T are small compared to the singlet 'binding energy' T_K. The reader is referred to the original papers [54] for the details. Here we only quote the result [48] for the imaginary part of the t-matrix at $|\omega|$ and T small compared to the Kondo temperature T_K,

$$-\pi\nu \operatorname{Im} T_s(\omega) = 1 - \frac{3\omega^2 + \pi^2 T^2}{2T_K^2}. \tag{6.26}$$

Substitution of (6.26) into (6.8) yields

$$G = G_0\left[1 - (\pi T/T_K)^2\right], \qquad T \ll T_K. \tag{6.27}$$

Accordingly, corrections to the conductance are quadratic in temperature—a typical Fermi liquid result [54]. The weak-coupling ($T \gg T_K$) and the strong-coupling ($T \ll T_K$) asymptotes of the conductance have a strikingly different structure. Nevertheless, since the Kondo effect is a crossover phenomenon rather than a phase transition [43–45, 47], the dependence $G(T)$ is a smooth and featureless [55] function throughout the crossover region $T \sim T_K$.

Finally, note that both equations (6.15) and (6.27) have been obtained here for the particle–hole symmetric model (5.12). This approximation is equivalent to neglecting the elastic co-tunnelling contribution to the conductance G_{el}. The asymptotes (6.15) and (6.27) remain valid [24] as long as $G_{el}/G_0 \ll 1$. The overall temperature dependence of the linear conductance in the middle of the Coulomb blockade valley is sketched in figure 4.

6.4. Beyond linear response

In order to study transport through a quantum dot away from equilibrium we add to the effective Hamiltonian (5.11)–(5.13) a term

$$H_V = \frac{eV}{2}\left(\hat{N}_L - \hat{N}_R\right) \tag{6.28}$$

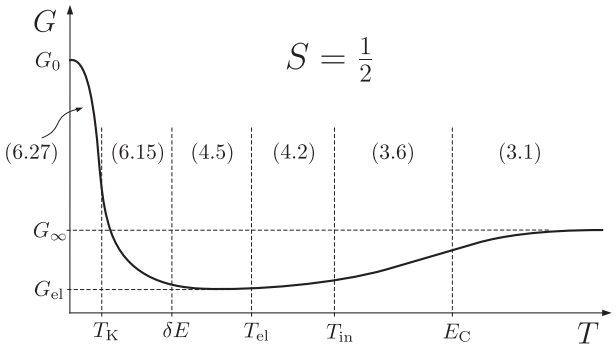

Figure 4. Sketch of the temperature dependence of the conductance in the middle of the Coulomb blockade valley with $S = 1/2$ on the dot. The numbers in brackets refer to the corresponding equations in the text.

describing a finite voltage bias V applied between the left (L) and right (R) electrodes. Here we will evaluate the current across the dot at arbitrary V but under the simplifying assumption that the dot–lead junctions are strongly asymmetric:

$$G_{\mathrm{L}} \ll G_{\mathrm{R}}.$$

Under this condition angle θ_0 in (6.6) is small, $\theta_0 \approx |t_{\mathrm{L}0}/t_{\mathrm{R}0}| \ll 1$. Expanding equation (6.7) to linear order in θ_0 we obtain

$$H_V(\theta_0) = \frac{eV}{2}\big(\hat{N}_2 - \hat{N}_1\big) + eV\theta_0 \sum_{ks}\big(\psi^\dagger_{1ks}\psi_{2ks} + \mathrm{H.c.}\big). \tag{6.29}$$

The first term in the rhs here can be interpreted as the voltage bias between the reservoirs of 1 and 2 particles (cf equation (6.28)), while the second term has an appearance of k-conserving tunnelling with very small (proportional to $\theta_0 \ll 1$) tunnelling amplitude.

Similar to equation (6.29), the current operator $\hat{I}$ (see (6.5)) splits naturally into two parts,

$$\hat{I} = \hat{I}_0 + \delta\hat{I},$$
$$\hat{I}_0 = \frac{\mathrm{d}}{\mathrm{d}t}\frac{e}{2}\big(\hat{N}_1 - \hat{N}_2\big) = -\mathrm{i}e^2V\theta_0 \sum_{ks}\psi^\dagger_{1ks}\psi_{2ks} + \mathrm{H.c.},$$
$$\delta\hat{I} = -e\theta_0\frac{\mathrm{d}}{\mathrm{d}t}\sum_{ks}\psi^\dagger_{1ks}\psi_{2ks} + \mathrm{H.c.}$$

It turns out that $\delta\hat{I}$ does not contribute to the average current in the leading (second) order in θ_0 [33]. The remaining contribution $I = \langle\hat{I}_0\rangle$ corresponds to tunnelling current between two bulk reservoirs containing 1 and 2 particles. Its evaluation yields [33]

$$\frac{\mathrm{d}I}{\mathrm{d}V} = G_0\frac{1}{2}\sum_s[-\pi\nu\,\mathrm{Im}\,T_s(eV)] \tag{6.30}$$

for the differential conductance across the dot at zero temperature. Here G_0 coincides with the small-θ_0 limit of equation (6.9). Now using equations (6.13), (6.14), and (6.26), we obtain

$$\frac{1}{G_0}\frac{\mathrm{d}I}{\mathrm{d}V} = \begin{cases} 1 - \dfrac{3}{2}\left(\dfrac{eV}{T_{\mathrm{K}}}\right)^2, & eV \ll T_{\mathrm{K}} \\ \dfrac{3\pi^2/16}{\ln^2(eV/T_{\mathrm{K}})}, & eV \gg T_{\mathrm{K}}. \end{cases} \tag{6.31}$$

Thus, a large voltage bias has qualitatively the same destructive effect on the Kondo physics as the temperature does. The result (6.31) remains valid as long as $T \ll eV \ll \delta E$. If the temperature exceeds the bias, $T \gg eV$, the differential conductance coincides with the linear conductance; see equations (6.15) and (6.27) above.

7. Kondo effect in quantum dots with large spin

If the dot's spin exceeds 1/2 [56–58], then, as discussed in section 5 above, both exchange constants J_γ in the effective Hamiltonian (5.2) are finite and positive. This turns out to have a dramatic effect on the dependence of the conductance in the Kondo regime on temperature T and on Zeeman energy B. Unlike the case of $S = 1/2$ on the dot (see figure 4), now the dependences on T and B are *non-monotonic*: initial increase of G is followed by a drop when the temperature is lowered [24, 59] at $B = 0$; the variation of G with B at $T = 0$ is similarly non-monotonic.

The origin of this peculiar behaviour is easier to understand by considering the B-dependence of the zero-temperature conductance [24]. We assume that the magnetic field $H_\parallel$ is applied *in the plane* of the dot. Such a field leads to the Zeeman splitting B of the spin states of the dot (see equation (6.23)), but barely affects the orbital motion of electrons.

At any finite B the ground state of the system is not degenerate. Therefore, the linear conductance at $T = 0$ can be calculated from the Landauer formula

$$G = \frac{e^2}{h} \sum_s \left| \mathbb{S}^2_{s;\mathrm{RL}} \right|, \tag{7.1}$$

which relates G to the amplitude of scattering $\mathbb{S}_{s;\mathrm{RL}}$ of an electron with spin s from lead L to lead R. The amplitudes $\mathbb{S}_{s;\alpha\alpha'}$ form a 2×2 scattering matrix $\hat{\mathbb{S}}_s$. In the basis of 'channels' (see equation (5.2)), this matrix is obviously diagonal, and its eigenvalues $\exp(2\mathrm{i}\delta_{\gamma s})$ are related to the scattering phase shifts $\delta_{\gamma s}$. The scattering matrix in the original $(R - L)$ basis is obtained from

$$\hat{\mathbb{S}}_s = \hat{U}^\dagger \mathrm{diag}\{\mathrm{e}^{2\mathrm{i}\delta_{\gamma s}}\}\hat{U},$$

where $\hat{U}$ is a matrix of a rotation by an angle θ_0; see equation (6.6). The Landauer formula (7.1) then yields

$$G = G_0 \tfrac{1}{2} \sum_s \sin^2(\delta_{1s} - \delta_{2s}), \qquad G_0 = \frac{2e^2}{h} \sin^2(2\theta_0), \tag{7.2}$$

which generalizes the single-channel expression (6.20).

Equation (7.2) can be further simplified for a particle–hole symmetric model (5.2). Indeed, in this case the phase shifts satisfy $\delta_{\gamma\uparrow} + \delta_{\gamma\downarrow} = 0$ (cf equation (6.22)), which suggests a representation

$$\delta_{\gamma s} = s\delta_\gamma.$$

Substitution into (7.2) then results in

$$G = G_0 \sin^2(\delta_1 - \delta_2). \tag{7.3}$$

If the spin on the dot S exceeds 1/2, then both channels of itinerant electrons participate in the screening of the dot's spin [42]. Accordingly, in the limit $B \to 0$ both phase shifts δ_γ approach the unitary limit value $\pi/2$; see figure 5. However, the increase of the phase shifts on lowering the field is characterized by two different energy scales. These scales, the Kondo

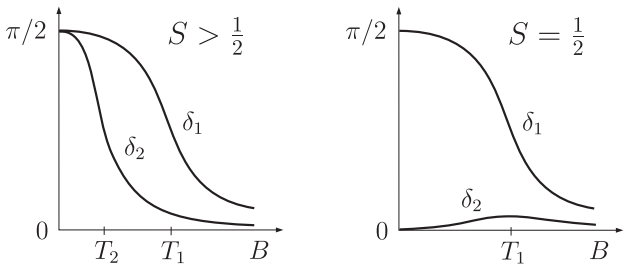

Figure 5. Dependence of the scattering phase shifts at the Fermi level on the magnetic field for $S > 1/2$ (left panel) and $S = 1/2$ (right panel).

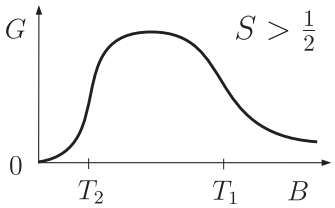

Figure 6. Sketch of the magnetic field dependence of the Kondo contribution to the linear conductance at zero temperature. The conductance as function of temperature exhibits a similar non-monotonic dependence.

temperatures T_1 and T_2, are related to the corresponding exchange constants in the effective Hamiltonian (5.2),

$$\ln\left(\frac{\Delta}{T_\gamma}\right) \sim \frac{1}{\nu J_\gamma},$$

so that $T_1 > T_2$ for $J_1 > J_2$. It is then obvious from equation (7.3) that the conductance across the dot is small both at weak ($B \ll T_2$) and strong ($B \gg T_1$) fields, but may become large ($\sim G_0$) at intermediate fields $T_2 \ll B \ll T_1$; see figure 6. In other words, the dependence of zero-temperature conductance on the magnetic field is non-monotonic.

This non-monotonic dependence is in sharp contrast with the monotonic increase of the conductance with lowering the field when $S = 1/2$. Indeed, in the latter case it is the channel whose coupling to the dot is the strongest that screens the dot's spin, while the remaining channel decouples at low energies [42]; see figure 5.

The dependence of the conductance on temperature $G(T)$ is very similar to $G(B)$.[8] For example, for $S = 1$ one obtains [24]

$$G/G_0 = \begin{cases} (\pi T)^2 \left(\dfrac{1}{T_1} - \dfrac{1}{T_2}\right)^2, & T \ll T_2 \\ \dfrac{\pi^2}{2}\left[\dfrac{1}{\ln(T/T_1)} - \dfrac{1}{\ln(T/T_2)}\right]^2, & T \gg T_1. \end{cases} \tag{7.4}$$

The conductance reaches its maximal value $G_{\max}$ at $T \sim \sqrt{T_1 T_2}$. The value of $G_{\max}$ can be found analytically for $T_1 \gg T_2$. For $S = 1$ the result reads [24]

$$G_{\max} = G_0\left[1 - \frac{3\pi^2}{\ln^2(T_1/T_2)}\right]. \tag{7.5}$$

[8] Note, however, that $\langle \psi_1^\dagger(t)\psi_2(t)\psi_2^\dagger(0)\psi_1(0)\rangle \neq \langle \psi_1^\dagger(t)\psi_1(0)\rangle\langle \psi_2(t)\psi_2^\dagger(0)\rangle$ at finite T. Therefore, unlike (6.20), equation (6.8) does not allow for a simple generalization to the two-channel case.

Consider now a Coulomb blockade valley with $N =$ even electrons and spin $S = 1$ on the dot. In a typical situation, the dot's spin in two neighbouring valleys (with $N \pm 1$ electrons) is $1/2$. Under the conditions of applicability of approximation (5.5), there is a single non-zero exchange constant $J_{N\pm1}$ for each of these valleys. If the Kondo temperatures T_K are the same for both valleys with $S = 1/2$, then $J_{N+1} = J_{N-1} = J_{\rm odd}$. Each of the two singly occupied energy levels in the valley with $S = 1$ is also singly occupied in one of the two neighbouring valleys. It then follows from equations (5.4)–(5.6) that the exchange constants $J_{1,2}$ for $S = 1$ satisfy

$$J_1 + J_2 = \tfrac{1}{2}\,(J_{N+1} + J_{N-1}) = J_{\rm odd}.$$

Since both J_1 and J_2 are positive, this immediately implies that $J_{1,2} < J_{\rm odd}$. Accordingly, both Kondo temperatures $T_{1,2}$ are expected to be smaller than T_K in the nearby valleys with $S = 1/2$.

This consideration, however, is not applicable when the dot is tuned to the vicinity of the singlet–triplet transition in its ground state [7, 8, 57, 58], i.e. when the energy gap Δ between the triplet ground state and the singlet excited state of an isolated dot is small compared to the mean level spacing δE. In this case the exchange constants in the effective Hamiltonian (5.2) should account for additional renormalization that the system's parameters undergo when the high-energy cut-off (the bandwidth of the effective Hamiltonian) D is reduced from $D \sim \delta E$ down to $D \sim \Delta \ll \delta E$ [60]; see also [49]. The renormalization enhances the exchange constants $J_{1,2}$. If the ratio $\Delta/\delta E$ is sufficiently small, then the Kondo temperatures $T_{1,2}$ for $S = 1$ may become of the same order [56, 58], or even significantly exceed [7, 8, 57] the corresponding scale T_K for $S = 1/2$.

In GaAs-based lateral quantum dot systems the value of Δ can be controlled by a magnetic field $H_\perp$ applied *perpendicular to the plane* of the dot [57]. Because of the smallness of the effective mass m^*, even a weak field $H_\perp$ has a strong orbital effect. At the same time, the smallness of the quasiparticle g-factor in GaAs ensures that the corresponding Zeeman splitting remains small [8]. The theory of the Kondo effect in lateral quantum dots in the vicinity of the singlet–triplet transition was developed in [61]; see also [62].

8. Discussion

In the simplest form of the Kondo effect considered in this review, a quantum dot behaves essentially as an artificial 'magnetic impurity' with spin S, coupled via exchange interaction to two conducting leads. The details of the temperature dependence $G(T)$ of the linear conductance across a lateral quantum dot depend on the dot's spin S. In the most common case of $S = 1/2$ the conductance in the Kondo regime monotonically increases with the decrease of temperature, potentially up to the quantum limit $2e^2/h$. Qualitatively (although not quantitatively), this increase can be understood from the Anderson impurity model in which the dot is described by a single energy level. In contrast, when spin on the dot exceeds $1/2$, the evolution of the conductance proceeds in two stages: the conductance first rises, and then drops again when the temperature is lowered.

In a typical experiment [3], one measures the dependence of the differential conductance on temperature T, Zeeman energy B, and dc voltage bias V. When one of these parameters is much larger than the other two, and is also large compared to the Kondo temperature T_K, the differential conductance exhibits a logarithmic dependence

$$\frac{1}{G_0}\frac{{\rm d}I}{{\rm d}V} \propto \left[\ln\frac{\max\{T, B, eV\}}{T_K}\right]^{-2}, \tag{8.1}$$

characteristic for the weak-coupling regime of the Kondo system. Consider now a zero-temperature transport through a quantum dot with $S = 1/2$ in the presence of a strong field $B \gg T_K$. In accordance with (8.1), the differential conductance is small compared to G_0 both for $eV \ll B$ and for $eV \gg B$. However, the calculation in the third order of perturbation theory in the exchange constant yields a contribution that diverges logarithmically at $eV = B$ [36]. The divergence appears because at $eV = B$ the scattered electron has just the right amount of energy to allow for a real transition with a flip of spin. However, the full development of resonance is inhibited by a finite lifetime of the excited spin state of the dot [41, 63]. As a result, the peak in the differential conductance at $eV \sim B$ is broader and lower [41] than the corresponding peak at zero bias in the absence of the field. Even though for $eV \sim B \gg T_K$ the system is clearly in the weak-coupling regime, a resummation of the perturbation series turns out to be a very difficult task, and the detailed shape of the peak is still unknown. This problem remains a subject of active research; see e.g. [64] and references therein.

One encounters similar difficulties in studies of the effect of a weak ac excitation of frequency $\Omega \gtrsim T_K$ applied to the gate electrode [65] on transport across the dot. In close analogy with the usual photon-assisted tunnelling [66], such perturbation is expected to result in the formation of satellites [67] at $eV = n\hbar\Omega$ (here n is an integer) to the zero-bias peak in the differential conductance. Again, the formation of the satellite peaks and the survival of the zero-bias peak in the presence of the ac excitation are limited by the finite-lifetime effects [68].

The spin degeneracy is not the only possible source of the Kondo effect in quantum dots. Consider, for example, a large dot connected by a single-mode junction to a conducting lead and tuned to the vicinity of the Coulomb blockade peak [22]. If one neglects the finite level spacing in the dot, then the two almost degenerate charge states of the dot can be labelled by a pseudospin, while the real spin plays the part of the channel index [22, 69]. This set-up turns out to be a robust realization [22, 69] of the symmetric (i.e. having equal exchange constants) two-channel $S = 1/2$ Kondo model [42]. The model results in a peculiar temperature dependence of the observable quantities, which at low temperatures follow power laws with manifestly non-Fermi-liquid fractional powers.

It should be emphasized that in the usual geometry, consisting of two leads attached to a small[9] Coulomb-blockaded quantum dot with $S = 1/2$, only the conventional Fermi-liquid behaviour can be observed at low temperatures. Indeed, in this case the two exchange constants in the effective exchange Hamiltonian (5.2) are vastly different, and their ratio is not tunable by conventional means; see the discussion in section 5 above. A way around this difficulty was proposed recently in [70]. The key idea is to replace one of the leads in the standard configuration by a very large quantum dot, characterized by a level spacing $\delta E'$ and a charging energy E'_C. At $T \gg \delta E'$, particle–hole excitations within this dot are allowed, and electrons in it participate in the screening of the smaller dot's spin. At the same time, as long as $T \ll E'_C$, the number of electrons in the large dot is fixed. Therefore, the large dot provides for a separate screening channel which does not mix with that supplied by the remaining lead. In this system, the two exchange constants are controlled by the conductances of the dot–lead and dot–dot junctions. A strategy for tuning the device parameters to the critical point characterized by the two-channel Kondo physics is discussed in [71].

Finally, we should mention that the description based on the universal Hamiltonian (2.13) is not applicable to large quantum dots subjected to a *quantizing* magnetic field $H_\perp$ [72, 73]. Such a field changes drastically the way the screening occurs in a confined droplet of a two-dimensional electron gas [74]. The droplet is divided into alternating domains containing compressible and incompressible electron liquids. In the metal-like compressible regions, the

[9] i.e. with appreciable level spacing.

screening is almost perfect. In contrast, the incompressible regions behave very much like insulators. In the case of lateral quantum dots, a large compressible domain may be formed near the centre of the dot. This domain is surrounded by a narrow incompressible region separating it from another compressible ring-shaped domain formed along the edges of the dot [75]. This system can be viewed as two concentric capacitively coupled quantum 'dots'—the core dot and the edge dot [72, 75]. When the leads are attached to the edge dot, the measured conductance is sensitive to its spin state: if the number of electrons in the edge dot is odd, then the conductance becomes large due to the Kondo effect [72]. Changing the field causes redistribution of electrons between the core and the edge, resulting in a striking chequerboard-like pattern of high- and low-conductance regions [72, 73]. This behaviour persists as long as the Zeeman energy remains small compared to the Kondo temperature. Note that compressible regions are also formed around an *antidot*—a potential hill in a two-dimensional electron gas in the quantum Hall regime [76]. Both Coulomb blockade oscillations and Kondo-like behaviour have been observed in these systems too [77].

9. Summary

The Kondo effect arises whenever a coupling to a Fermi gas induces transitions within otherwise degenerate ground state multiplet of an interacting system. Both coupling to a Fermi gas and interactions are naturally present in a nanoscale transport experiment. At the same time, many nanostructures can be easily tuned to the vicinity of a degeneracy point. This is why the Kondo effect in its various forms often influences the low-temperature transport in meso-and nanoscale systems.

In this article we reviewed the theory of the Kondo effect in transport through quantum dots. A Coulomb-blockaded quantum dot behaves in many aspects as an artificial 'magnetic impurity' coupled via exchange interaction to two conducting leads. The Kondo effect in transport through such an 'impurity' manifests itself in the lifting of the Coulomb blockade at low temperatures, and, therefore, can be unambiguously identified. Quantum dot systems not only offer a direct access to transport properties of an artificial impurity, but also provide one with a broad arsenal of tools to tweak the impurity properties, unmatched in conventional systems. The characteristic energy scale for the intradot excitations is much smaller than the corresponding scale for natural magnetic impurities. This allows one to induce degeneracies in the ground state of a dot which are more exotic than just the spin degeneracy. This is only one of many possible extensions of the simple model discussed in this review.

Acknowledgments

The research at the University of Minnesota was supported by NSF grants DMR02-37296, and EIA02-10736.

References

[1] Kouwenhoven L P *et al* 1997 *Mesoscopic Electron Transport* ed L L Sohn *et al* (Dordrecht: Kluwer) p 105
Kastner M A 1992 *Rev. Mod. Phys.* **64** 849
Meirav U and Foxman E B 1996 *Semicond. Sci. Technol.* **11** 255
Kouwenhoven L P and Marcus C M 1998 *Phys. World* **11** 35
[2] Joyez P *et al* 1997 *Phys. Rev. Lett.* **79** 1349
Devoret M and Glattli C 1998 *Phys. World* **11** 29
[3] Goldhaber-Gordon D *et al* 1998 *Nature* **391** 156
Cronenwett S M, Oosterkamp T H and Kouwenhoven L P 1998 *Science* **281** 540
Schmid J *et al* 1998 *Physica* B **256–258** 182
[4] Kouwenhoven L and Glazman L 2001 *Phys. World* **14** 33
[5] Kondo J 1964 *Prog. Theor. Phys.* **32** 37
[6] Tarucha S *et al* 2000 *Phys. Rev. Lett.* **84** 2485

Kouwenhoven L P, Austing D G and Tarucha S 2001 *Rep. Prog. Phys.* **64** 701
[7] Sasaki S *et al* 2000 *Nature* **405** 764
[8] Pustilnik M *et al* 2001 *Lect. Notes Phys.* **579** 3 (*Preprint* cond-mat/0010336)
[9] Nygård J, Cobden D H and Lindelof P E 2000 *Nature* **408** 342
Liang W, Bockrath M and Park H 2002 *Phys. Rev. Lett.* **88** 126801
[10] Park J *et al* 2002 *Nature* **417** 722
Liang W *et al* 2002 *Nature* **417** 725
[11] Knorr N *et al* 2002 *Phys. Rev. Lett.* **88** 096804
Manoharan H C *et al* 2000 *Nature* **403** 512
Madhavan V *et al* 1998 *Science* **280** 567
Chen W *et al* 1999 *Phys. Rev.* B **60** R8529
Li J T *et al* 1998 *Phys. Rev. Lett.* **80** 2893
[12] Berry M V 1985 *Proc. R. Soc.* A **400** 229
Altshuler B L and Shklovskii B I 1986 *Sov. Phys.—JETP* **64** 127
[13] Beenakker C W J 1997 *Rev. Mod. Phys.* **69** 731
Alhassid Y 2000 *Rev. Mod. Phys.* **72** 895
[14] Mehta M L 1991 *Random Matrices* (New York: Academic)
[15] Altshuler B L *et al* 1997 *Phys. Rev. Lett.* **78** 2803
Agam O *et al* 1997 *Phys. Rev. Lett.* **78** 1956
Blanter Ya M 1996 *Phys. Rev.* B **54** 12807
Blanter Ya M and Mirlin A D 1998 *Phys. Rev.* B **57** 4566
Blanter Ya M, Mirlin A D and Muzykantskii B A 1997 *Phys. Rev. Lett.* **78** 2449
Aleiner I L and Glazman L I 1998 *Phys. Rev.* B **57** 9608
[16] Kurland I L, Aleiner I L and Altshuler B L 2000 *Phys. Rev.* B **62** 14886
[17] Aleiner I L, Brouwer P W and Glazman L I 2002 *Phys. Rep.* **358** 309
[18] Berry M V 1977 *J. Phys. A: Math. Gen.* **10** 2083
Blanter Ya M and Mirlin A D 1997 *Phys. Rev.* E **55** 6514
Blanter Ya M, Mirlin A D and Muzykantskii B A 2001 *Phys. Rev.* B **63** 235315
Mirlin A D 2000 *Phys. Rep.* **326** 259
[19] Ziman J M 1972 *Principles of the Theory of Solids* (Cambridge: Cambridge University Press)
[20] Brouwer P W, Oreg Y and Halperin B I 1999 *Phys. Rev.* B **60** R13977
Baranger H U, Ullmo D and Glazman L I 2000 *Phys. Rev.* B **61** R2425
[21] Potok R M *et al* 2003 *Phys. Rev. Lett.* **91** 016802
Folk J A 2001 *Phys. Scr.* T **90** 26
Lindemann S *et al* 2002 *Phys. Rev.* B **66** 195314
[22] Matveev K A 1995 *Phys. Rev.* B **51** 1743
[23] Flensberg K 1993 *Phys. Rev.* B **48** 11156
[24] Pustilnik M and Glazman L I 2001 *Phys. Rev. Lett.* **87** 216601
[25] Kulik I O and Shekhter R I 1975 *Sov. Phys.—JETP* **41** 308
Glazman L I and Shekhter R I 1989 *J. Phys.: Condens. Matter* **1** 5811
[26] Giaever I and Zeller H R 1968 *Phys. Rev. Lett.* **20** 1504
Zeller H R and Giaever I 1969 *Phys. Rev.* **181** 789
[27] Averin D V and Nazarov Yu V 1990 *Phys. Rev. Lett.* **65** 2446
[28] Abrikosov A A 1988 *Fundamentals of the Theory of Metals* (Amsterdam: North-Holland)
[29] Aleiner I L and Glazman L I 1996 *Phys. Rev. Lett.* **77** 2057
[30] Silva A, Oreg Y and Gefen Y 2002 *Phys. Rev.* B **66** 195316
Baltin R and Gefen Y 1999 *Phys. Rev. Lett.* **83** 5094
[31] Glazman L I and Raikh M E 1988 *JETP Lett.* **47** 452
Ng T K and Lee P A 1988 *Phys. Rev. Lett.* **61** 1768
[32] van der Wiel W G *et al* 2000 *Science* **289** 2105
Ji Y, Heiblum M and Shtrikman H 2002 *Phys. Rev. Lett.* **88** 076601
[33] Glazman L I and Pustilnik M 2003 *New Directions in Mesoscopic Physics (Towards Nanoscience)* ed R Fazio *et al* (Dordrecht: Kluwer) p 93 (*Preprint* cond-mat/0302159)
[34] Duke C B 1969 *Tunneling in Solids* (New York: Academic)
Rowell J M 1969 *Tunneling Phenomena in Solids* ed E Burstein and S Lundqvist (New York: Plenum) p 385
[35] Wyatt A F G 1964 *Phys. Rev. Lett.* **13** 401
Logan R A and Rowell J M 1964 *Phys. Rev. Lett.* **13** 404
[36] Appelbaum J A 1966 *Phys. Rev. Lett.* **17** 91

Appelbaum J A 1967 *Phys. Rev.* **154** 633
[37] Anderson P W 1966 *Phys. Rev. Lett.* **17** 95
[38] Fiete G A *et al* 2002 *Phys. Rev.* B **66** 024431
[39] Schrieffer J R and Wolff P A 1966 *Phys. Rev.* **149** 491
[40] Silvestrov P G and Imry Y 2000 *Phys. Rev. Lett.* **85** 2565
[41] Meir Y, Wingreen N S and Lee P A 1993 *Phys. Rev. Lett.* **70** 2601
[42] Nozières P and Blandin A 1980 *J. Physique* **41** 193
[43] Coleman P 2002 *Lectures on the Physics of Highly Correlated Electron Systems* ed F Mancini (New York: American Institute of Physics) p 79 (*Preprint* cond-mat/0206003)
Hewson A S 1997 *The Kondo Problem to Heavy Fermions* (Cambridge: Cambridge University Press)
[44] Anderson P W 1997 *Basic Notions of Condensed Matter Physics* (Reading, MA: Addison-Wesley)
[45] Wilson K G 1975 *Rev. Mod. Phys.* **47** 773
[46] Glazman L I, Hekking F W J and Larkin A I 1999 *Phys. Rev. Lett.* **83** 1830
[47] Tsvelick A M and Wiegmann P B 1983 *Adv. Phys.* **32** 453
Andrei N, Furuya K and Lowenstein J H 1983 *Rev. Mod. Phys.* **55** 331
[48] Affleck I and Ludwig A W W 1993 *Phys. Rev.* B **48** 7297
[49] Pustilnik M and Glazman L I 2001 *Phys. Rev.* B **64** 045328
[50] Abrikosov A A 1965 *Physics* **2** 5
Abrikosov A A 1969 *Sov. Phys.—Usp.* **12** 168
[51] Newton R G 2002 *Scattering Theory of Waves and Particles* (Mineola: Dover)
[52] Anderson P W 1970 *J. Phys. C: Solid State Phys.* **3** 2436
[53] Anderson P W, Yuval G and Hamann D R 1970 *Phys. Rev.* B **1** 4464
[54] Nozières P 1974 *J. Low Temp. Phys.* **17** 31
Nozières P 1978 *J. Physique* **39** 1117
[55] Costi T A, Hewson A C and Zlatić V 1994 *J. Phys.: Condens. Matter* **6** 2519
[56] Schmid J *et al* 2000 *Phys. Rev. Lett.* **84** 5824
[57] van der Wiel W G 2002 *Phys. Rev. Lett.* **88** 126803
[58] Kogan A *et al* 2003 *Phys. Rev.* B **67** 113309
[59] Izumida W, Sakai O and Shimizu Y 1998 *J. Phys. Soc. Japan* **67** 2444
[60] Eto M and Nazarov Yu V 2000 *Phys. Rev. Lett.* **85** 1306
Pustilnik M and Glazman L I 2000 *Phys. Rev. Lett.* **85** 2993
[61] Golovach V N and Loss D 2003 *Europhys. Lett.* **62** 83
Pustilnik M, Glazman L I and Hofstetter W 2003 *Phys. Rev.* B **68** 161303(R)
[62] Pustilnik M, Avishai Y and Kikoin K 2000 *Phys. Rev. Lett.* **84** 1756
[63] Losee D L and Wolf E L 1969 *Phys. Rev. Lett.* **23** 1457
[64] Rosch A, Costi T A, Paaske J and Wölfle P 2003 *Phys. Rev.* B **68** 014430
Paaske J, Rosch A and Wölfle P 2003 *Preprint* cond-mat/0307365
[65] Elzerman J M *et al* 2000 *J. Low Temp. Phys.* **118** 375
[66] Tien P K and Gordon J P 1963 *Phys. Rev.* **129** 647
[67] Hettler M H and Schoeller H 1995 *Phys. Rev. Lett.* **74** 4907
[68] Kaminski A, Nazarov Yu V and Glazman L I 1999 *Phys. Rev. Lett.* **83** 384
[69] Matveev K A 1991 *Sov. Phys.—JETP* **72** 892
[70] Oreg Y and Goldhaber-Gordon D 2003 *Phys. Rev. Lett.* **90** 136602
[71] Pustilnik M *et al* 2004 *Phys. Rev.* B **69** 115316
[72] Keller M *et al* 2001 *Phys. Rev.* B **64** 033302
Stopa M *et al* 2003 *Phys. Rev. Lett.* **91** 046601
[73] Maurer S M *et al* 1999 *Phys. Rev. Lett.* **83** 1403
Sprinzak D *et al* 2002 *Phys. Rev. Lett.* **88** 176805
Fühner C *et al* 2002 *Phys. Rev.* B **66** 161305(R)
Keyser U F *et al* 2003 *Phys. Rev. Lett.* **90** 196601
[74] Beenakker C W J 1990 *Phys. Rev. Lett.* **64** 216
Chang A M 1990 *Solid State Commun.* **74** 871
Chklovskii D B, Shklovskii B I and Glazman L I 1992 *Phys. Rev.* B **46** 4026
[75] McEuen P L *et al* 1992 *Phys. Rev.* B **45** 11419
Evans A K, Glazman L I and Shklovskii B I 1993 *Phys. Rev.* B **48** 11120
[76] Goldman V J and Su B 1995 *Science* **267** 1010
[77] Kataoka M *et al* 1999 *Phys. Rev. Lett.* **83** 160
Kataoka M *et al* 2002 *Phys. Rev. Lett.* **89** 226803